Journal of Solid State Chemistry 183 (2010) 3002–3009

Contents lists available at ScienceDirect

Journal of Solid State Chemistry

journal homepage: www.elsevier.com/locate/jssc

Solubility and release of fenbufen intercalated in Mg, Al and Mg, Al, Fe layered double hydroxides (LDH): The effect of Eudragit® S 100 covering

M. del Arco, A. Fernández, C. Martín, V. Rives *

GIR-QUESCAT, Departamento de Química Inorgánica, Universidad de Salamanca, 37008 Salamanca, Spain

ARTICLE INFO

Article history:
Received 13 July 2010
Received in revised form
4 October 2010
Accepted 11 October 2010
Available online 19 October 2010

Keywords:
Fenbufen
LDH
Layered double hydroxide
Eudragit® S100
Drug release

ABSTRACT

Following different preparation routes, fenbufen has been intercalated in the interlayer space of layered double hydroxides with Mg^{2+} and Al^{3+} or Mg^{2+}, Al^{3+} and Fe^{3+} in the layers. Well crystallized samples were obtained in most of the cases (intercalation was not observed by reconstruction of the MgAlFe matrix), with layer heights ranging between 16.1 and 18.8 Å. The presence of the LDH increases the solubility of fenbufen, especially when used as a matrix. The dissolution rate of the drug decreases when the drug is intercalated, and is even lower in those systems containing iron; release takes place through ionic exchange with phosphate anions from the solution. Preparation of microspheres with Eudragit® S 100 leads to solids with an homogeneous, smooth surface with efficient covering of the LDH surface, as drug release was not observed at pH lower than 7.

1. Introduction

Non-steroid anti-inflammatory drugs (NSAIDs) constitute a heterogeneous group of drugs with similar therapeutical (analgesic, antiinflamatory, and antipyretic) properties, but differing in their efficiency and relative toxicity. Fenbufen is an NSAID derived from propionic acid, used to treat rheumatoid-arthritis and osteoarthritis, but its used is somewhat limited by the undesired collateral effects affecting gastrointestinal tract and central nervous system. One of the main challenges currently facing the pharmaceutical industry is to improve the effectivity of the drugs and to diminish their undesired effects. More precisely, in the case of orally delivered drugs the presence of excipients plays an important role on the release of the active species and its absorption rate by the organism.

Layered double hydroxides (LDHs), also known as anionic clays, are biocompatible inorganic materials formed by divalent metal cation hydroxide layers with the brucite structure, with a partial, isomorphical substitution by trivalent cations, leading to a positively charged layer, which is balanced by the presence of hydrated anions in the interlayer, thus leading a stacking of positive and negative charged layers [1]. LDHs have been recently used to prepare organic/inorganic hybrids, by intercalating anionic drug molecules in the interlayer space, thus becoming protected against changes originated by damping, light or heat, the inorganic solid acting as a matrix to prepare systems with controlled drug release. Different organic anionic have been intercalated in the interlayer space of LDHs, namely, DNA [2–6], amino acids [7–10], drugs to reduce cholesterol levels [11], anticancer [12], antibiotics [13], anticoagulants like heparine, with a short life time [14], etc. These studies have addressed the advantages of the drug-LDH systems agains the pure drugs. Ambrogi et al. [15] have reported an increase in the solubility of indomethacine when this rather insoluble drug is intercalated. Panda et al. [11] have studied the protection agains light, damp, and ultraviolet radiation of pravastatin and fluvastatin when intercalated. Choi et al. [12] have reported a larger effectivity of the drug-LDH (methotrexate and 5-fluorouracil) than the very toxic pure drugs, used in chemotherapy.

Different authors have previously studied the intercalation of several antiinflamatory drugs and the effect of intercalation on the solubility and dissolution rate of the drug [16–25].

On designing a modified release formulation for a given drug, one of the challenges to be addressed is to control the place where release will take place. As LDHs are readily dissolved in an acidic medium, dissolution in the stomach will take place immediately unless the hybrid is covered with a polymer to prevent such a dissolution. A rather few number of studies have reported on drug-LDH systems covered with pH-dependent polymers [26,27].

We here report the preparation of LDHs with Mg and Al, or Mg, Al, and Fe in the brucite-like layers, containing intercalated fenbufen, prepared by different methods. The samples have been characterized using different techniques, and the solubility and release rate of intercalated fenbufen are also studied. Finally, some of the samples here prepared have been covered with Eudragit® S 100

* Corresponding author. Fax: +34923294574.
E-mail address: vrives@usal.es (V. Rives).

0022-4596/$ - see front matter © 2010 Elsevier Inc. All rights reserved.
doi:10.1016/j.jssc.2010.10.017

(insoluble at pH lower than 7) following two procedures, namely, simple dispersion or forming microspheres to study the effect of the preparation method on the drug release rate.

2. Experimental

2.1. Samples preparation

Samples with Mg and Al, or Mg, Al, and Fe in the brucite-like layers and with intercalated fenbufen were prepared by direct coprecipitation, anionic exchange (from a sample with chloride in the interlayer) and reconstruction (from a calcined sample originally containing carbonate in the interlayer). In all cases, calculated amounts of the corrersponding metal clorides were mixed to prepare solids with the desired molar ratios ($M^{2+}/M^{3+}=2$, $Fe^{3+}/(Fe^{3+}+Al)=0.1$).

2.1.1. Samples prepared by coprecipitation

The starting salt solutions was prepared adding 1.26 g (6.2 mmol) of $MgCl_2 \cdot 6H_2O$ (Fluka) and 0.75 g (3.1 mmol) of $AlCl_3 \cdot 6H_2O$ (Panreac) or 0.675 g (2.79 mmol) of $AlCl_3 \cdot 6H_2O$ and 0.084 g (0.51 mmol) of $FeCl_3 \cdot 6\,H_2O$ (Panreac) to 50 mL of decarbonated water. Once perfectly dissolved, this solution was slowly added to a solution prepared by dissolving 0.8 g (3.1 mmol) of fenbufen (Sigma–Aldrich) in 100 mL of decarbonated water, at pH 8 after adding the required amount of KOH (Panreac). Once addition was complete the suspension formed was magnetically stirred at 70 °C for 2 days under N_2 atmosphere. The suspension was then centrifuged and the solid washed several times with decarbonated water. The solid was filtered and dried in a desiccator with $CaCl_2$, yielding samples named cFb (containing Mg and Al) and cFeFb (containing Mg, Al, and Fe).

2.1.2. Samples prepared by anion exchange

The precursors used were LDHs with chloride in the interlayer (named as MgAl/Cl and MgAlFe/Cl), had been prepared following the conventional precipitation method described elsewhere [28], and were kept in solution until used, i.e., they were not isolated from the mother liquor. A portion of 3 g (11.79 mmol) of fenbufen dissolved in 150 mL of decarbonated water containing the amount of KOH required for complete dissolution of the drug, was added to 100 mL of a suspension of MgAl/Cl (3.2 g) or MgAlFe/Cl (4.72 g). The suspension thus obtained was stirred under nitrogen atmosphere at 70 °C for 7 days. It was then centrifuged and washed several times with decarbonated water. The solids (named eFb and eFeFb) were stored in the desiccator under vacuum.

2.1.3. Samples prepared by reconstruction

The precursors used were LDHs with carbonate in the interlayer, sample C (containing Mg and Al) and sample FeC (containing Mg, Al, and Fe) [28]. A portion of 2 g of the precursor, C, or FeC, was calcined at 5 °C/min up to 500 °C and this temperature maintained for 4 h under a nitrogen flow. The solid obtained was added to a solution containing 2.5 g (9.83 mmol) of fenbufen dissolved in decarbonated water where the required amount of KOH had been added to reach a pH of 8 for complete dissolution of NSAID. The suspension formed was maintained at 70 °C for 2 days (under reflux) The solid was filtered, washed several times with decarbonated water, dried, and kept in a desiccators with $CaCl_2$ under vacuum, leading to samples named rFb and rFeFb.

2.1.4. Polymer covering

Two methods have been followed to prepare the polymer-covered samples, simple dispersion of the active principle in the polymeric material or immobilization in microspheres. In the first case, 2 g of Eudragit® S 100 was dissolved in 30 mL of ethanol and then 0.2 g of the drug was added. The resulting suspension was vigorously stirred for 2 h at 70 °C and then it was added to 400 mL of vigorously stirred water. The solid was filtered and dried at 80 °C, leading to sample named as DFb. For the second method, also used to cover sample eFb, the microspheres were prepared by the solvent extraction–evaporation method in an oil/water (O/W) emulsion, widely used for encapsulation of hardly soluble active components [29]. An organic phase was first prepared by dissolving 1 g of Eudragit® S 100 (supplied by Pharma Polymers, Degussa) in a solution containing 10 mL ethanol and 5 mL dichloromethane. Then 100 mg of sample was added and the suspensión was sonicated (Selecta) 10 min. The organic phase was added to 200 mL of the aqueous one, W, formed by a 75% w/v mixture of polyvinyl alcohol in bidistilled water; the suspension was kept at 40 °C for 3 h while stirred at 500 rpm. The microspheres were washed several times with an aqueous solution of HCl (pH=5), filtered and dried, leading to samples MFb and MeFb.

2.2. Experimental techniques

Element chemical analyses for Mg, Al, and Fe were carried out in Servicio General de Análisis Químico Aplicado (University of Salamanca, Spain) in a model ULTIMA-2 ICP-OES spectrophotometer from Jovin Yvon, after dissolving the samples in nitric acid. C and N were analyzed in an Elemental Analyzer from Leco, model CHNS 932.

The powder X-ray diffraction patterns (PXRD) were collected on a Siemens D-500 diffractometer using Cu$K\alpha$ radiation ($\lambda=1.54050$ Å). The Fourier-Transform Infrared spectra (FT-IR) were recorded in a Perkin-Elmer FT-1730 instrument using the KBr pellet technique; 100 scans were averaged to improve the signal-to-noise ratio, at a nominal resolution of 4 cm^{-1}. Differential thermal analyses (DTA) and thermogravimetric analyses (TGA) were measured on DTA7 and TGA7 instruments from Perkin-Elmer, respectively. The analyses were carried out in flowing (30 mL/min) oxygen from L'Air Liquide (Spain) at a heating rate of 10 °C/min.

The morphology of the microspheres was assessed by Scanning Electron Microscopy (SEM) using a digital Zeiss DSM 940 Scanning Microscope connected to a Scan Converter DSC-1024 G Sony. The samples were covered with a gold film using a BIO-RAD ES100 Sen Coating System.

Solubility and release studies were carried out in a temperature-controlled bath (Selecta, model Unitronic 320 OR) with a stirrer (Velp Scientifica DHL). The dissolution-rate studies were carried out using a Hanson SR6-SRII 6 flask dissolution test station following the USP (United States Pharmacopeia) and BP (British Pharmacopeia) protocols; using method 2, as described in RFE 3.0 (Real Farmacopea Española). The samples were stirred at 100 ± 2 rpm and the temperature was 37 ± 0.2 °C. The amount of dissolved drug in the solution was determined by ultraviolet–visible (UV–V) spectroscopy in a Hewlett Packard UV–V 8452 spectrophotometer.

2.3. Solubility studies

Solubility studies of fenbufen were carried out under experimental conditions as close as possible to those of the gastrointestinal tract, in terms of pH and the medium, (enzyme-free): buffer solutions at pH=1.2 (HCl/KCl) for gastric fluid, and 4.5 (KH_2PO_4/Na_2HPO_4/HCl) and 6.8 (Na_2HPO_4/NaH_2PO_4) for intestinal fluid. Studies were carried out 37 ± 0.5 °C (to simulate a living organism) and a stirring rate of 100 ± 2 rpm, simulating peristalsis and also allowing a maximum discrimination to detect products with

a small yield in vivo. Solubility studies were carried out under saturation conditions, adding a given amount of sample containing 0.5, 0.75, or 1.0 g of Fb to 500 mL of buffer solution at pH 1.2, 4.5, or 6.8, respectively. The samples (Fb and eFb) were kept at the stirring and temperature conditions given above for 24 h, with 5 mL of solution extracted at given time intervals. The same amount of buffer solution was added after each extraction to maintain a constant volume. The extracted solution was then filtered using a Millex HV Millipore with a pore diameter of 0.45 μm. Phosphate buffer solution was added as required in order to reach a pH of 7.8. The concentration of fenbufen in the solution was determined by UV–V spectroscopy, using the Lambert–Beer law and the absorbance measured at 285 nm using a reference plot. All experiments were conducted in triplicate.

2.4. Release-rate studies in vitro

These studies were carried out under the experimental conditions described in BP 2005, using rigid gelatine capsules (ACOFAR), no. 00. The solution media were 900 mL of phosphate buffer (pH 7.5). The amount of sample used was chosen to correspond to 250 mg of drug. Aliquots of 5 mL were extracted at given time intervals and 5 mL of buffer solution added to replace it and maintain a constant volume. The withdrawn aliquot was then filtered (Millex HV Millipore, pore diameter=0.45 μm). The amount of drug released was determined as for the solubility studies.

2.5. Kinetic studies

The results from the solubility and in vitro release-rate studies were treated to determine the process parameters using an independent analysis model ($t_{50\%}$, $t_{85\%}$ and mean dissolution time (MDT)) and a dependent analysis model, adjusting the experimental data to different kinetic models (zero order, first-order, Hixson–Crowell, and Higuchi and Weibull) [30] using Win Nonlin 3.0 software (Pharsight Corporation Software); the Weibull model was chosen to adjust the experimental data on the basis of the minimum values obtained for the Akaike Information Criteria (AIC). The statistical analysis was carried out using the ANOVA method (analysis of variance), assuming a value of $p<0.05$ to be significant. All experiments were conducted in triplicate.

2.6. Determination of microspheres drug content

Once the microspheres were covered with the polymer, the production yield, corresponding to the percentage of covered sample, with respect to the total amount of drug (or drug+carrier) and polymer used, was determined. The fenbufen content, or encapsulation ability, has been determined by UV–V spectroscopy at $\lambda=285$ nm. To remove the polymer, a given amount of sample was added to a 0.1 M NaOH solution; in the case of sample MeFb the basic treatment was extended for 48 h, to be sure a total exchange of carbonate for interlayer fenbufen. The drug content was calculated as

$$\%\text{Drug content} = (\text{amount of entrapped drug}/\text{weight of microspheres}) \times 100$$

The yield of encapsulation efficiency was calculated as

$$\text{EE}(\%) = (\text{actual loading}/\text{theoretical loading}) \times 100$$

In these samples, the release study has been carried out following a standard method for formulations with enteric covering, as described in USP29-NF25. The measurements have been carried out under conditions simulating the course of the drug through the gastrointestinal tract, in pH gradient. The essay was started at pH 1,2; after 2 h the pH was changed to 6.8 and 2 h later it was increased up to 7.5, which was maintained until the end of the essay. Switch of pH required less than 5 min and HCl (2 M) or NaOH (2 M) were used to fix the pH at 6.8 ± 0.05 and pH 7.5 ± 0.05. A thermostatised bath (37 ± 0.5 °C) was used, with a paddle type apparatus (60 rpm). Dissolution essays have been carried out in an analogous way to those used for the uncovered samples.

3. Results and discussion

3.1. Uncovered samples

3.1.1. Characterization

Element chemical analysis for Mg, Al, Fe, and C for all samples prepared, as well as some informative atomic ratios calculated for the former data are shown in Table 1. The M^{2+}/M^{3+} molar ratio is essentially identical to that in the precursor solids [21,28] or to the ratio between the amounts of salts used to prepare the samples, suggesting that intercalation of the drug molecules has taken place through a topotactic process, without destruction of the layered structure, and that precipitation of the cations has been complete. This ratio, however, is larger to the expected value or larger than for the precursors in those samples containing iron, indicating that the Mg^{2+}/Fe^{3+} substitution in the layers is larger than expected. The Fe^{3+}/Al^{3+} ratio is about twice than expected for simple cFeFb, and the M^{3+}/drug ratio is also larger than expected (one), except for sample cFeFB, always assuming that all carbon detected corresponds to intercalated fenbufen. These results suggest that together with the anionic form of fenbufen, other anionic species (unexchanged chloride species, or hydroxyl arising from the basic medium), are present to balance the positive charge of the layers. Unfortunately, these results prevent from determining the precise formulae of the compounds prepared [31,32]. The drug content ranges from 31% to 44% (weight), values similar to those by other authors for LDHs with drugs in the interlayer [15,19–23,33].

The powder X-ray diffraction (PXRD) diagrams of all samples are included in Fig. 1. All they are characteristic of well crystallized LDHs with the hydrotalcite-type structure. The three first sharp diffraction maxima (from the low diffraction angle side) are due to diffraction by planes (003), (006), and (009), respectively, assuming a rhombohedral stacking of the layers; usually the relative

Table 1
Result from element chemical analysis, specific surface areas and d_{003} values of the samples prepared.

Sample	Al[a]	Mg[a]	Fe[a]	C (%)	M^{2+}/M^{3+}	Fe/M^{3+}[b]	M^{3+}/drug[b]	Drug (%)	d_{003} (Å)
eFb	5.5	9.4	–	34.0	1.9	–	1.1	40.6	22.36
cFb	5.8	9.4		37.2	1.8	–	1.1	36.2	23.61
rFb	5.6	9.5		33.2	1.9	–	1.2	39.0	23.18
eFeFb	5.4	16.6	1.5	22.0	3	0.1	1.7	31.4	20.9
cFeFb	3.4	9.8	1.6	34.5	2.6	0.2	0.9	44.4	21.9

[a] Weight percentage.
[b] Molar ratio.

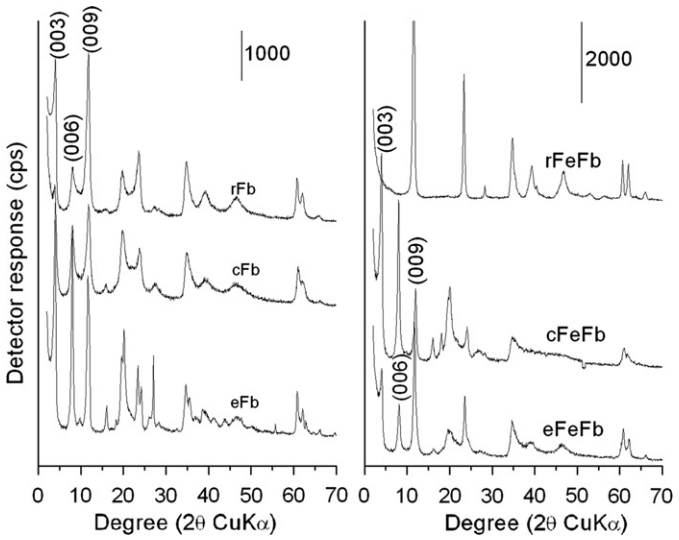

Fig. 1. Powder X-ray diffraction diagrams for the MgAl-fenbufen (left) and MgAlFe-fenbufen (right) LDHs.

intensities of these lines decrease as the diffraction angle increases. The larger intensity of the (009) line can be related to the volume of the anion, or to a high electron density in the interlayer [34–35]. The values determined for parameter d_{003} are included in Table 1. These are markedly larger than those corresponding to LDHs with intercalated chloride or carbonate (around 7.8 Å) [21,23], indicating that substitution (or intercalation) has actually taken place and the fenbufen anion has been successfully intercalated. Incorporation of iron does not give rise to changes in the relative intensities of the recorded maxima nor in their positions, and the observed differences should be related to the different preparation procedures followed. The maxima are sharper and are better defined for the samples prepared by anionic exchange and no diffraction lines due to crystalline fenbufen are recorded.

Maxima at 7.6 and 3.8 Å are, however, recorded for samples rFb and cFb, these positions being coincident, within experimental error, with those ascribed to diffraction by planes (003) and (006), respectively, of samples containing carbonate, hydroxyl or chloride, suggesting the presence of a biphasic system. The presence of carbonate could arise from defective calcination or contamination from atmospheric CO_2 during handling of the samples, due to the strongly basic character of these solids. Chloride and hydroxyl anions exist in the reaction medium during preparation of the samples, and can be hosted in the interlayer, contributing to balance the positive charge of the layers, in agreement with the element chemical analysis data. Fortunately for the aim of this study, neither chloride nor hydroxyl is toxic and so the samples would be still useful for pharmacological applications. The differences observed in the relative intensities of the diffraction lines for these samples are due to the fact that sample eFb is much more crystalline than sample rFb. Although crystalline fenbufen shows diffraction maxima in the 20–30° (2θ) range, no diffraction maximum which could be attributed to fenbufen is recorded for our samples. The PXRD diagram for sample rFeFb is similar to the carbonate precursor (FeC), indicating that the presence of iron prevents intercalation of the drug by the reconstruction method, probably because of the larger acidity of the iron-containing samples, thus displaying a larger affinity for carbonate.

The molecular size of fenbufen, as determined using Chem. Office Ultra 8.0 2004 (http://www.camsoft.com) software is 14.76 Å [25]. As the width of the brucite-like layers is 4.8 Å [36], the height available for inclusion of fenbufen, as determined from the PXRD data, ranges from 16.1 to 16.8 Å for the different samples. These values are larger than that calculated for fenbufen, but similar to those reported by other authors for hydrotalcites containing intercalated NSAID molecules (naproxen, indomethacin, etc.) [16,37–39]. Some authors claim that the drug molecules are oriented perpendicular to the brucite-like layers forming a monolayer in the interlayer space [40], while others [17] have proposed that the orientation of the molecules depends on the preparation conditions. In any case, the molecules are oriented to maximize the interaction between the carboxylate groups and the brucite-like layers [16,17,20,41]. Wei et al. [37] have proposed that the drug molecules are oriented perpendicular to the brucite-like layers but, in addition, a layer of water molecules is located between the organic anions and the inorganic layers, as on adding to the largest drug dimension the van der Waals radii of hydrogen and oxygen and the width of the water molecule, the value obtained is very similar to the experimental one for samples with intercalated fenbufen. From the values calculated, then, for the gallery height and the data reported for similar systems, the small differences found for our samples are probably related to small differences in their hydration degree [38,39,42] or tilting of the interlayer fenbufen species [43].

The FT-IR spectra of representative samples, as well as that of fenbufen, are included in Fig. 2. No significant differences are found, whichever the preparation procedure or the layer composition. The spectrum of fenbufen shows many sharp, intense, bands due to the aromatic rings, and the methyl, carbonyl, and carboxylate groups.

Bands characteristic of CH and OH stretching modes are recorded between 4000 and 2500 cm^{-1}. A weak band characteristic of substituted aromatic rings is recorded close to 2000 cm^{-1}. The precise positions of the bands are given in the figure. The stretching mode of the C=O unit in the carboxylic and cetonic groups gives rise to two bands at 1710 and 1677 cm^{-1}, respectively. The bands due to the stretching C–C modes of the aromatic rings are recorded between 1770 and 1450 cm^{-1} and between 1470 and 1430 cm^{-1} the band originated by the deformation mode of the methyl group [25,44]. Owing to the close coincidence between the positions of the bands originated by different stretching and/or deformation modes it results extremely difficult a precise ascription of all bands recorded for fenbufen.

In the spectra of the samples where is intercalated in the interlayer space of the LDH structure, the fenbufen originated bands are recorded (less intense than for pure fenbufen), together with the bands due to the LDH structure. Some changes are also observed, thus, the band due to the free carboxylic group

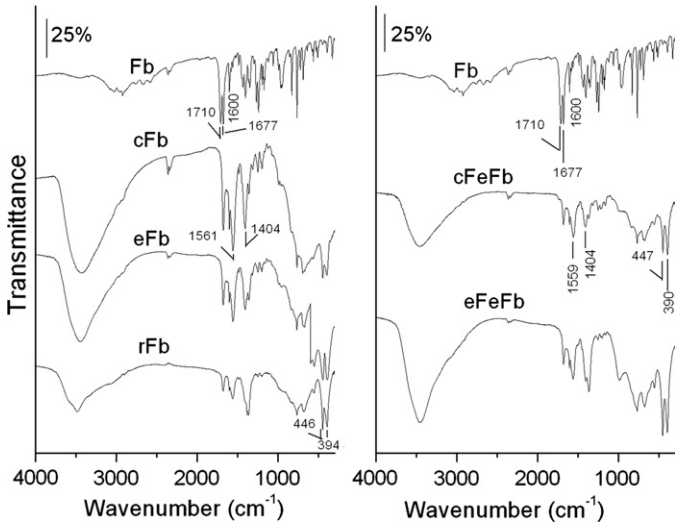

Fig. 2. FT-IR spectra of fenbufen (Fb) and of samples with intercalated fenbufen.

disappears (as expected because of the intercalation of the fenbufen molecule in its anionic form). This finding confirms also the absence of externally adsorbed free fenbufen molecules. In addition, two bands due to the carboxylate group are recorded at 1561 and 1404 cm^{-1}, corresponding to the antisymmetric and symmetric COO stretching modes, respectively. The presence of appreciable amounts of carbonate could have been concluded from its typical, intense, band somewhat below 1400 cm^{-1}, but it is not observed in the spectra of our samples, as they could be masked by the intense bands of the drug. Chloride anions do not give rise, by themselves, to IR bands, and those from the hydroxyl group would be included in those due to layer hydroxyl groups and of water molecules. The other bands due to the drug are recorded in the same positions as for free fenbufen; regarding the bands due to the inorganic phase, a broad band recorded between 3490 and 3590 cm^{-1} is ascribed to the stretching mode of hydroxyl groups, both from the brucite-like layers and the interlayer water molecules. The broadness of this band arises from the existence of hydrogen-bonded hydroxyl groups, with different strength between the layer hydroxyl groups and the interlayer water molecules. The band at ca. 1610 cm^{-1} is due to the deformation mode of water molecules [44,45]. The bands recorded below 600 cm^{-1} are due to vibrations of the "rigid" brucite-like layers, involving Mg, Al (and Fe), and OH groups.

Thermal evolution of the samples is similar to those reported in the literature for LDHs intercalated with organic species, with no significant differences among the samples prepared by the different methods here tested, nor for the different LDH hosts used. The DTA-TG diagram for sample cFb, shown in Fig. 3, shows an endothermic effect between 120 and 130 °C due to release of adsorbed and interlayer water molecules. A broad, rather weak, exothermic effect is recorded between 200 and 375 °C, probably due to combustion of fenbufen existing in the border of the crystallites [17]. The sharp, intense, exothermic effect centered at 550 °C is due to combustion of fenbufen existing in the interlayer space. This effect is recorded at 491 °C for sample eFeFb, Fig. 3; this shift can be probably related to the different amounts of drug existing in these two samples, which in some way should control its stability in the interlayer and/or to formation of iron oxide, which could behave as catalysts for total combustion of the drug. Dehydroxylation of the brucite-like layers is expected also in this temperature range as an endothermic effect, but their intensity should be markedly lower than that of the combustion effects and appear cancelled in the diagrams by the strong effects of the oxidative degradation of the drugs [46].

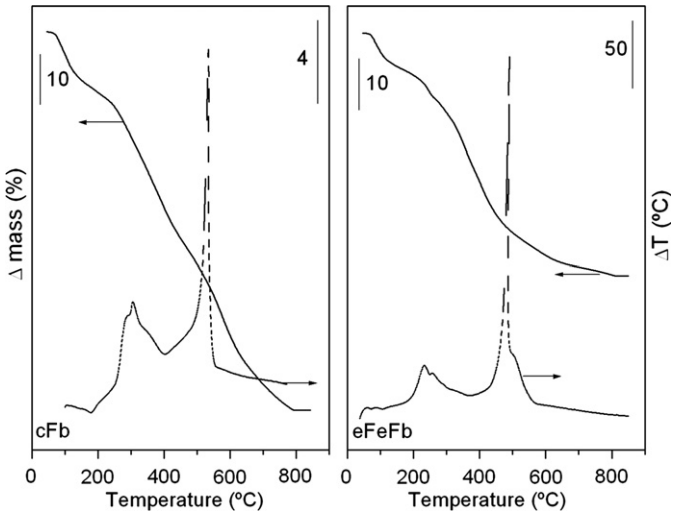

Fig. 3. DTA/TG diagrams for samples cFb (left) and eFeFb (right).

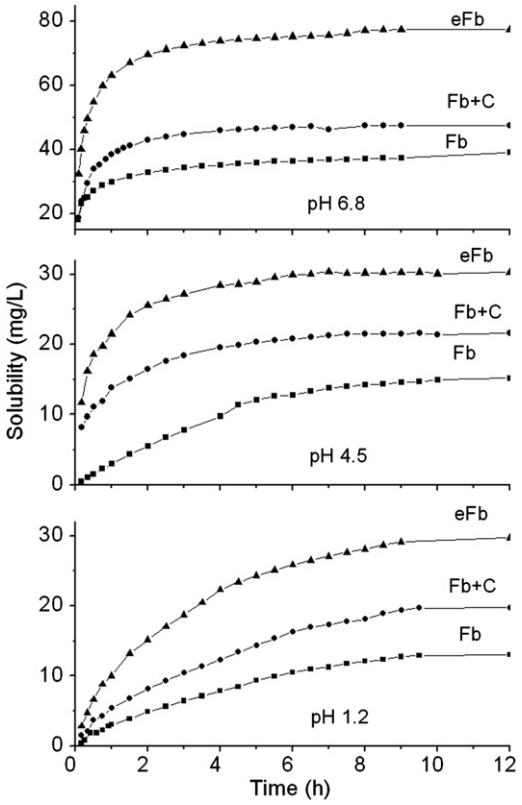

Fig. 4. Apparent solubility of Fb from eFb, in comparison with Fb and from the physical mixture (Fb+C) at pH 1.2, 4.5, and 6.8.

3.1.2. *Solubility studies*

Solubility measurements were carried out following the protocol described above. Our aim was to check if intercalation of the drugs in the interlayer improved the solubility at pH values simulating the actual conditions of the gastrointestinal tract. Changes in the solubility with time for pure and intercalated Fb in the Mg, Al LDH at the three values of pH tested are plotted in Fig. 4. The curves for the physical mixture of hydrotalcite with interlayer carbonate and fenbufen are also included in this figure. As it can be here seen, whichever the pH value, the solution curves corresponding to pure fenbufen are below those corresponding to the LDH-containing samples, suggesting that the presence of LDH increases the solubility of the drug, especially when the drug is intercalated. Therefore, addition of hydrotalcite (sample C) to Fb increases the solubility by 51%, 62%, and 21% at pH 1.2, 4.5, and 6.8, respectively. The presence of hydrotalcite also increases the dissolution rate; so, a concentration of 12 g/L is reached at pH 1.2 for pure fenbufen after 10 h, while only 4.3 h are needed to reach this same concentration when using the Fb+C mixture, and 1.5 h for the intercalated drug. Previous studies have shown that the presence of LDH leads to an increase in the solubility of scarcely soluble anti-inflammatory drugs [15,22]. The increased solubility observed for the physical mixture can be due to the increase of pH because of the LDH [22], for those samples containing intercalated fenbufen the enhacement of drug solubility could presumably be explained by the lack in cristallinity of intercalated drugs that are directly released in ionic form by dissolution of hydrotalcite in acid medium [15].

Solubility was almost the same at pH 1.2 and 4.5 for all three formulations used (Fb, Fb+C, and eFb), being much lower than at pH 6.8. For the drug, solubility at pH 6.8 is three times that measured at pH 1.2.

The powder X-ray diffraction diagrams (not shown) of the undissolved residue after tests at $t_{100\%}$ for all three formulations indicate that at pH 1.2 and 4.5 hydrotalcite is dissolved and only weak diffraction maxima of fenbufen are recorded. However, diffraction maxima due to fenbufen and phosphate-intercalated hydrotalcite are recorded for the residue of the tests carried out at pH 6.8. These results are similar to those reported previously for intercalation and dissolution of mefenamic acid [22].

Data for solubility of fenbufen have been mathematically treated, analyzing the effect of pH and the presence of hydrotalcite on the solubility, following two models, namely, the independent model and the dependent model one. The average values for the parameters and constants calculated for the model to which a best fit is reached are given in Table 2. The increase in solubility and dissolution rate observed as the pH increases gives rise to changes in the parameters measured. Therefore, minimum values for AUC and maximum values for MDT, $t_{50\%}$ and $t_{85\%}$ are reached at pH 1.2. When pH is increased, AUC increases and the other parameters decrease, minimum values being reached at pH 6.8, suggesting that for the formulations tested this is the most favorable pH. Differences in solubilities for pH 1.2 and 4.5 are very small, but the changes in the parameters are statistically significant.

The effect of hydrotalcite as an additive or as a host matrix gives also rise to changes in the parameters. Values for $t_{50\%}$, $t_{85\%}$, and MDT decrease by 37%, 17%, and 21%, respectively, at pH 1.2 for the intercalated drug, but only 10%, 6.3%, and 8% for the physical mixture. Changes are more evident at pH 4.5. Statistically non-significant differences are found between pure fenbufen and the physical mixture at pH 6.8.

Statistical criteria analyzing the goodness of the fit (AIC and SS) for the different parameter-dependent models show that the best model is the Weibull one; the fit parameter values are included in Table 2. Values for t_d, $t_{50\%}$ and MDT change similarly at pH 1.2 and 4.5, while at pH 6.8 the values for parameter t_d are close to those for $t_{50\%}$, but not for TMD, probably because at this pH the differences among these values are not statistically significant.

3.1.3. Release study

In vitro dissolution of fenbufen from samples eFb and eFeFb has been studied following the USP protocol; the results are summarized in Fig. 5A. For both matrices containing Mg and Al, or Mg, Al, and Fe in the brucite-like layers the dissolution curve for intercalated fenbufen is below those for pure fenbufen and the physical mixture, indicating that the presence of the matrices decreases the dissolution rate. The curves corresponding to the physical mixtures (carbonate-containing hydrotalcites and drug) are similar to each other and to that for pure fenbufen. Partial Al/Fe substitution in the layers gives rise to a decrease in the release rate of fenbufen. For instance, 95% of fenbufen is dissolved after 1 h from sample eFb, but only 59% from sample eFeFb. The presence of iron, however, does not give rise to any change in the dissolution data for the physical mixtures.

In a similar way to the analysis of the solubility data, dissolution rate data have been also fitted to the kinetic models above listed, in order to determine the role of the presence of hydrotalcite and the chemical composition of the layers; the data obtained are shown in Table 3. The differences observed among the parameters determined by the different methods are not statistically significant regarding pure fenbufen and the physical mixture, as expected from the shapes of the corresponding dissolution curves, but, on comparing $t_{50\%}$, $t_{85\%}$, and MDT for the pure and the intercalated drug, increases of 286%, 620%, and 330%, respectively, for these parameters, are observed.

The presence of iron in the layers gives rise to a significant ($p < 0.05$) decrease in the amount of dissolved drug and in the dissolution rate, as concluded from these parameters. From the fitting of the experimental data to the parameter-dependent models, it can be observed that the best fit is obtained for the Weibull model; the values for the corresponding parameters are also shown in Table 3; they change similarly to the equivalent parameters calculated by the parameter-dependent model.

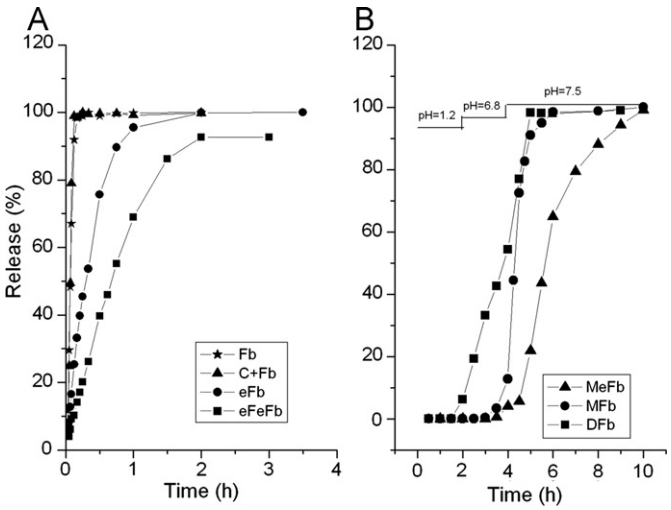

Fig. 5. Release studies of intercalated fenbufen: (A) uncovered samples and (B) samples covered with Eudragit® S 100.

Table 2
Solubility and fitting parameters for the independent and Weibull models.

pH	Sample	SOLUB (mg/L)	Independent model parameters			Weibull parameters			Weibull	
			$t_{50\%}$ (h)	AUC	MTD (h)	Q_∞ (mg)	t_d (h)	ß	AIC	SS
1.2	Fb	13.02 ± 0.19	3.07 ± 0.10	266 ± 1.3.56	3.60 ± 0.05	13.84	4.36	1.05	35.84	39.50
	Fb+C	19.72 ± 0.29	2.75 ± 0.13	408 ± 16.10	3.31 ± 0.03	21.05	4.11	0.96	54.68	55.09
	eFb	29.69 ± 0.28	1.93 ± 0.07	629 ± 15.78	2.85 ± 0.06	30.87	3.91	0.85	30.01	33.28
4.5	Fb	15.18 ± 0.17	2.89 ± 0.05	312 ± 9.34	3.49 ± 0.04	15.79	3.74	1.23	10.14	13.55
	Fb+MC	21.55 ± 0.14	0.45 ± 0.02	488 ± 17.78	1.43 ± 0.09	22.65	1.09	0.51	36.07	39.48
	eFb	30.27 ± 0.18	0.29 ± 0.02	697 ± 14.87	1.03 ± 0.03	30.94	0.66	0.51	27.39	30.79
6.8	Fb	39.10 ± 0.14	0.24 ± 0.06	881 ± 18.15	1.59 ± 0.05	40.06	0.36	0.30	31.09	34.62
	Fb+C	47.41 ± 0.15	0.16 ± 0.09	1107 ± 11.03	0.70 ± 0.04	47.75	0.35	0.47	21.4	24.94
	eFb	77.42 ± 0.10	0.14 ± 0.04	1801 ± 17.65	0.75 ± 0.03	77.56	0.32	0.45	31.87	35.40

Table 3
Fitting parameters for the independent and Weibull models for the dissolution studies.

Sample	Independen model parameters				Weibull parameters			Weibull	
	$t_{50\%}$ (h)	$t_{85\%}$ (h)	AUC	MDT	Q_∞ (mg)	t_d (h)	β	AIC	SS
Fb	0.07 ± 0.01	0.09 ± 0.01	853.86 ± 15.26	0.01 ± 0.02	248.47	0.073	3.3	57.05	78.75
Fb+C	0.07 ± 0.02	0.11 ± 0.01	855.14 ± 13.99	0.10 ± 0.01	248.46	0.079	2.25	50.61	52.31
eFb	0.27 ± 0.02	0.65 ± 0.02	787.49 ± 17.09	0.43 ± 0.08	253.84	0.394	1.13	75.92	77.84
Fb+FeC	0.07 ± 0.02	0.12 ± 0.02	857.00 ± 17.73	0.12 ± 0.04	248.55	0.087	1.72	75.79	77.71
eFeFb	0.64 ± 0.02	1.47 ± 0.14	659.81 ± 24.59	0.79 ± 0.02	237.24	0.845	1.15	92.34	94.46

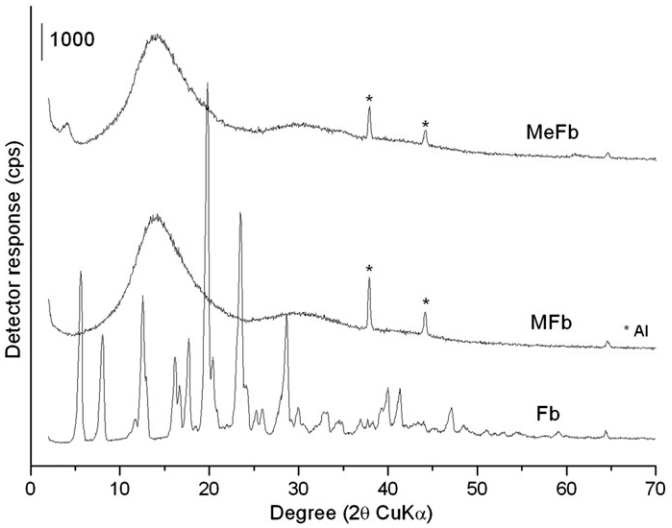

Fig. 6. Powder X-ray diffraction diagrams of fenbufen and of the fenbufen-LDH composites coated by the polymer in the form of microspheres.

3.2. Samples coated with polymer

3.2.1. Characterization

The powder X-ray diffraction diagrams of fenbufen and of the fenbufen-LDH composites coated by the polymer in the form of microspheres are shown in Fig. 6. Only diffraction maxima due to Eudragit® S 100 [17] are recorded for sample Mfb, without maxima due to crystalline fenbufen. However, for the MeFb sample, in addition to the maxima due to the polymer, a low intense diffraction maximum due to (003) planes of the fenbufen-LDH phase is also recorded, indicating that during the preparation of these composites the integrity of the phases is preserved [17].

Scanning electron microscopy has been applied to analyze the morphology of the microspheres, to insight also in their size and internal structure. The SEM micrographs of fenbufen samples covered by both methods and of intercalated fenbufen microspheres are included in Fig. 7. As it can be here observed, the surface is smooth and homogeneous in the microspheres prepared by the extraction–evaporation method, but showing a certain degree if inhomogeneity when fenbufen is covered with Eudragit® S 100 by simple dispersion of the active principle in the polymer solution. The diameter of the microspheres is in the range 50–60 μm, which is well adequate for oral administration, and their surface is smooth and homogeneous.

Yield values for preparation of these microspheres are always larger than 75%, and encapsulation efficiency range from 85% to 94%. The powder XRD pattern (not shown) of sample MFb show diffraction lines due to the polymer [26], while in that for sample MeFb the lines recorded suggest the presence of two phases, namely, one corresponding to the eFb hydrotalcite and the other to the polymer, suggesting that the identity of the phases is maintained during the preparation process.

3.2.2. Dissolution tests

Dissolution tests for the delayed release formulations have been carried out under experimental conditions as close as possible to the gastrointestinal tract (2 h at pH 1.2, 2 h at pH 6.8, and 5 h at pH 7.5); the curves corresponding to samples DFb, MFb, and MeFb are included in Fig. 5B. No dissolution of fenbufen is observed at pH 1.2, but after 2 h at pH 6.8, for sample DFb, 54% has been released, indicating that the simple dispersion method does not lead to a good nor efficient covering of the particles, as Eudragit® S 100 is only dissolved at pH close to 7 or above. Release of Fb in the covered, intercalated formulation is slower than in the microspheres of the pure drug, as to release the drug located in the interlayer an ionic exchange with phosphate anions in the solution is first required, similarly to the findings reported for the uncovered formulations; all (100%) fenbufen is released after 5 h at pH 7.5. These results are different from those previously reported by Li et al. [26] and Ambrogi et al. [27] for samples containing fenbufen or diclofenac intercalated in LDHs and covered with Eudragit. Li et al. [26] find a release only of 67% after 9 h for fenbufen intercalated in a Mg, Al hydrotalcite covered with Eudragit (without forming microspheres), suggesting that interaction of the carboxylate groups of the polymer with the surface of the hydrotalcite microcrystals inhibits deintercalation of the drug and dissolution of the polymer. A similar process has been claimed by Ambrogi et al. [27] for release of diclofenac, with a maximum release of 78% after 8 h, the amount of drug released being proportional to the amount of polymer used for preparing the covering. The differences found between our results and those previously reported in the literature are undoubtedly related to the covering method and with the release mechanism of the drug from the interlayer space. Li et al. [26] have suggested that complete dissolution of the polymer and deintercalation of fenbufen can be inhibited by the interaction between the carboxylate groups of the polymer and the surface of the LDH particles. However, these same authors also report that only 40% and 60% of fenbufen is released from uncovered LiAl and MgAl LDHs, respectively, probably this being also the maximum amount able to be released when covered with the polymer. For our samples, the drug is completely released from the interlayer, both for uncovered and polymer-covered samples; provided they are kept time enough in suspension to allow dissolution of the polymer, and to permit ionic exchange with the phosphate anions of the buffer medium.

4. Conclusions

The different methods here used to intercalate fenbufen in MgAl and MgAlFe LDHs lead to samples with drug loadings ranging from 31% to 44% (w/w). The presence of iron inhibits intercalation of fenbufen following the reconstruction method.

The presence of the LDH increases the solubility and dissolution rate of fenbfen at the three pH values tested, the maximum values being reached at pH 6.8; the best fit of the experimental data corresponds to the model of Weibull.

The dissolution rate of fenbufen is lower when intercalated, due to the exchange process which takes place through ionic exchange with the phosphate anions of the buffer solution; this process is

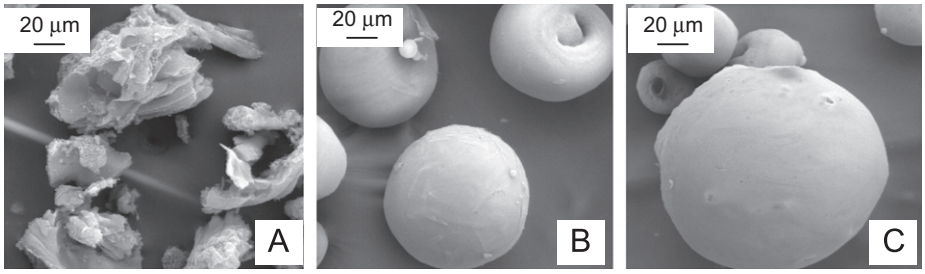

Fig. 7. SEM micrographs of samples (A) DFb, (B) MFb, and (C) MeFb.

slower in the samples containing iron, probably because of a stronger interaction between the drug and the layers, which is more acidic in this case than in the absence of iron.

Formation of microspheres covered with the polymer guaranties stability of the system and no dissolution at pH below 7.

Acknowledgments

Financial support from MICINN (Grant MAT2009-08526) and ERDF was greatly acknowledged.

References

[1] V. Rives (Ed.), Layered Double Hydroxides: Present and Future, Nova Science Publishing Co. Inc., New York, 2001.
[2] S.Y. Kwak, Y.J. Jeong, J.S. Park, J.H. Choy, Solid State Ionics 151 (2002) 229.
[3] Z.P. Xu, T.L. Walker, K. Liu, H.M. Cooper, G.Q.M. Lu, P.F. Barlett, Int. J. Nanomed. 2 (2007) 163.
[4] J.H. Choy, S.Y. Kwak, J.S. Park, Y.J. Jeong, J. Portier, J. Am. Chem. Soc. 121 (1999) 1399.
[5] L. Mohanambe, S. Vasudevan, Inorg. Chem. 44 (2005) 2128.
[6] J.H. Choy, S.J. Jung, J.M. Oh, M. Park, J. Jeong, Y.K. Kang, O.J. Han, Biomaterials 25 (2004) 3059.
[7] Q. Yuan, M. Wei, D.G. Evans, X. Duan, J. Phys. Chem. B 108 (2004) 12381.
[8] T. Hibino, Chem. Mater. 16 (2004) 5482.
[9] H. Nakayama, N. Wada, M. Tsuhako, Int. J. Pharm. 269 (2004) 469.
[10] S. Aisawa, S. Takahashi, W. Ogasawara, Y. Umetsu, E. Narita, J. Solid State Chem. 162 (2001) 52.
[11] H.S. Panda, R. Srivastava, D. Bahadur, J. Phys. Chem. B 113 (2009) 15090.
[12] S.J. Choi, J.M. Oh, J.H. Choy, J. Phys. Chem. Solids 69 (2008) 1528.
[13] G. Carja, Y. Kameshima, G. Ciobanu, H. Chiriac, K. Okada, Micron 40 (2009) 147.
[14] Z. Gu, A.C. Thomas, Z.P. Xu, J.H. Campbell, G.Q. Lu, Chem. Mater. 20 (2008) 3715.
[15] V. Ambrogi, G. Fardella, G. Grandolini, M. Nocchetti, L. Perioli, J. Pharm. Sci. 92 (2003) 1407.
[16] A.I. Khan, L.X. Lei, A.J. Norquist, D. O'Hare, Chem. Commun. 22 (2001) 2342.
[17] B. Li, J. He, D.G. Evans, X. Duan, Appl. Clay Sci. 27 (2004) 199.
[18] U. Costantino, V. Ambrogi, M. Nocchetti, L. Perioli, Microporous Mesoporous Mater. 107 (2008) 149.
[19] M. del Arco, S. Gutiérrez, C. Martín, V. Rives, J. Rocha, J. Solid State Chem. 177 (2004) 3954.
[20] M. del Arco, E. Cebadera, S. Gutiérrez, C. Martín, M.J. Montero, V. Rives, J. Rocha, M.A. Sevilla, J. Pharm. Sci. 93 (2004) 1649.
[21] M. del Arco, A. Fernández, C. Martín, V. Rives, Appl. Clay Sci. 36 (2007) 133.
[22] M. del Arco, A. Fernández, C. Martín, M.L. Sayalero, V. Rives, Clay Miner. 43 (2008) 255.
[23] M. del Arco, A. Fernández, C. Martín, V. Rives, Appl. Clay Sci. 42 (2009) 538.
[24] D. Carriazo, M. del Arco, C. Martín, C. Ramos, V. Rives, Microporous Mesoporous Mater. 130 (2010) 229.
[25] D. Carriazo, M. del Arco, A. Fernández, C. Martín, V. Rives, J. Pharm. Sci. 99 (2010) 3372.
[26] B. Li, J. He, D.G. Evans, X. Duan, Int. J. Pharm. 287 (2004) 89.
[27] V. Ambrogi, L. Perioli, M. Ricci, L. Pulcini, M. Nocchetti, S. Giovagnoli, C. Rossi, Microporous Mesoporous Mater. 115 (2008) 405.
[28] D. Carriazo, M. del Arco, C. Martín, V. Rives, Appl. Clay Sci. 37 (2007) 231.
[29] C. Remuñan López, M.J. Alonso Fernández, Tecnología Farmacéutica. Volumen I: Aspectos Fundamentales de los sistemas farmacéuticos y operaciones básicas, in: J.L.Vila Jato (Ed.), Síntesis, Madrid1997, p. 592.
[30] P. Costa, J.M. Sousa, Eur. J. Pharm. Sci. 13 (2001) 123.
[31] S. Carlino, M.J. Hudson, J. Mater. Chem. 5 (1995) 1433.
[32] S. Carlino, M.J. Hudson, S.W. Husain, J.A. Knowles, Solid State Ionics 84 (1996) 117.
[33] V. Ambrogi, G. Fardella, G. Grandolini, L. Perioli, Int. J. Pharm. 220 (2001) 23.
[34] T. Kwon, T.J. Pinnavaia, Chem. Mater. 1 (1989) 381.
[35] T. Hibino, A. Tsunashima, Chem. Mater. 9 (1997) 2082.
[36] M.A. Drezdzon, Inorg. Chem. 27 (1988) 4628.
[37] M. Wei, S.X. Shi, J. Wang, Y. Li, X. Duan, J. Solid State Chem. 177 (2004) 2534.
[38] G. Fardella, L. Perioli, U. Costantino, M. Nocchetti, V. Ambrogi, G. Grandolini, Proc. Int. Symp. Control Rel. Bioact. Mater. 24 (1997) 1033.
[39] G. Fardella, V. Ambrogi, L. Perioli, G. Grandolini, Proc. Int. Symp. Control Rel. Bioact. Mater. 25 (1998) 774.
[40] L. Latterini, M. Nocchetti, G.G. Aloisi, U. Costantino, F. Elisei, Inorg. Chem. Acta 360 (2007) 728.
[41] H. Zhang, K. Zou, S. Guo, X. Duan, J. Solid State Chem. 179 (2006) 1792.
[42] G.D. Moggridge, P. Parent, G. Tourillon, Clays Clay Miner. 42 (1994) 462.
[43] M. Meyn, K. Beneke, G. Lagaly, Inorg. Chem. 29 (1990) 5201.
[44] L.J. Bellamy (Ed.), Chapman & Hall, London, 1975.
[45] J.T. Kloprogge, R.L. Frost, in: V. Rives (Ed.), Layered Double Hydroxides: Present and Future, Nova Science Publishing Co. Inc, New York2001, p. 139 Chapter. 5.
[46] V. Rives, in: V. Rives (Ed.), Layered Double Hydroxides: Present and Future, Nova Science Publishing Co. Inc, New York2001, p. 115 (Chapter 4).